Equivalent genetic roles for *bmp7/snailhouse* and *bmp2b/swirl* in dorsoventral pattern formation

Bettina Schmid[1],*, Maximilian Fürthauer[2],*, Stephanie A. Connors[1], Jamie Trout[1], Bernard Thisse[2], Christine Thisse[2] and Mary C. Mullins[1],‡

[1]University of Pennsylvania School of Medicine, Department of Cell and Developmental Biology, 1211 BRBII/III, Philadelphia, PA 19104-6058, USA
[2]Institut de Génétique et de Biologie Moléculaire et Cellulaire, CNRS/INSERM/ULP, BP 163, 67404 Illkirch Cedex, CU de Strasbourg, France
*These authors contributed equally to this work.
‡Author for correspondence (e-mail: mullins@mail.med.upenn.edu)

SUMMARY

A bone morphogenetic protein (BMP) signaling pathway acts in the establishment of the dorsoventral axis of the vertebrate embryo. Here we demonstrate the genetic requirement for two different Bmp ligand subclass genes for dorsoventral pattern formation of the zebrafish embryo. From the relative efficiencies observed in Bmp ligand rescue experiments, conserved chromosomal synteny, and isolation of the zebrafish *bmp7* gene, we determined that the strongly dorsalized *snailhouse* mutant phenotype is caused by a mutation in the *bmp7* gene. We show that the original *snailhouse* allele is a hypomorphic mutation and we identify a *snailhouse/bmp7* null mutant. We demonstrate that the *snailhouse/bmp7* null mutant phenotype is identical to the presumptive null mutant phenotype of the strongest dorsalized zebrafish mutant *swirl/bmp2b*, revealing equivalent genetic roles for these two Bmp ligands. Double mutant *snailhouse/bmp7; swirl/bmp2b* embryos do not exhibit additional or stronger dorsalized phenotypes, indicating that these Bmp ligands do not function redundantly in early embryonic development. Furthermore, overexpression experiments reveal that Bmp2b and Bmp7 synergize in the ventralization of wild-type embryos through a cell-autonomous mechanism, suggesting that Bmp2b/Bmp7 heterodimers may act in vivo to specify ventral cell fates in the zebrafish embryo.

Key words: Dorsoventral, Pattern formation, Bmp7, Bmp2b, TGFβ, Zebrafish

INTRODUCTION

Dorsoventral axis formation in vertebrates and invertebrates depends on a conserved signal transduction pathway mediated by secreted ligands of the TGFβ superfamily, the BMPs (reviewed in De Robertis and Sasai, 1996; Ferguson, 1996). In dorsoventral axis formation, a gradient of BMP activity is hypothesized to form along the axis and specify different cell fates in a concentration-dependent manner. In vertebrates the gradient of BMP activity is thought to be generated through the diffusion into lateral and ventral regions of dorsally expressed BMP antagonists, which can directly bind and inhibit BMP activity (reviewed in Cho and Blitz, 1998).

BMP ligands are processed from a preprotein and dimerize to form mature ligands. Within the Bmp family there are several distinct subclasses: *bmp2* and *bmp4* are most closely related to *Drosophila decapentaplegic* (*dpp*), whereas *bmp7*, also referred to as OP-1, belongs to a *bmp5,6,7* subclass and is most closely related to *glass bottom boat-60A* in *Drosophila* (reviewed in Hogan, 1996). Bmp dimers bind two distinct classes of transmembrane serine-threonine receptor kinases, type I and type II, which have been suggested to form a tetrameric receptor complex binding two Bmp dimers. This activated receptor complex phosphorylates downstream Smad proteins, which then translocate into the nucleus and regulate transcription of downstream target genes (reviewed in Massagué, 1998). Genetic analyses in the zebrafish demonstrate a requirement for the *smad5*, *chordin* and *bmp2b* genes in dorsoventral axis formation (Hild et al., 1999; Kishimoto et al., 1997; Nguyen et al., 1998b; Schulte-Merker et al., 1997).

The requirement for different Bmp ligands during early vertebrate embryogenesis has been difficult to address. Overexpression studies in *Xenopus* reveal that Bmp2, Bmp4 and Bmp7 have very similar biological potentials in the early embryo (Hawley et al., 1995; Nishimatsu and Thomsen, 1998). Due to the potential promiscuity in heterodimerization of both Bmp receptors and Bmp ligands (Hazama et al., 1995), overexpression of dominant-negative mutants for these Bmp components may display a lack of specificity and interfere with signaling by several Bmps. In the mouse a small fraction of *bmp4* mutants display a lack of

ventroposterior mesodermal derivatives, consistent with a role in dorsoventral patterning (Winnier et al., 1995). However, redundancy in Bmp function and/or a maternal Bmp contribution has been suggested to account for the lack of early patterning defects observed in *bmp2* and *bmp7* mutant mouse embryos (Dudley et al., 1995; Dudley and Robertson, 1997; Zhang and Bradley, 1996). Therefore, the characterization of zebrafish mutants of these Bmp ligands allows one to address the presently unresolved question of the contribution of different Bmp ligands to early dorsoventral patterning of a vertebrate embryo.

Here we demonstrate that the strongly dorsalized zebrafish *snailhouse* (*snh*) mutant is caused by a mutation in the *bmp7* gene. We show that the null *snh/bmp7* mutant phenotype is indistinguishable from the *swirl* (*swr*)/*bmp2b* null phenotype. Moreover, *snh/bmp7; swr/bmp2b* double mutant embryos do not exhibit a stronger dorsalized phenotype than the single mutants, demonstrating that *bmp2b* and *bmp7* in the zebrafish are equally required to specify ventral cell fates. Furthermore, coinjection of *bmp2b* and *bmp7* mRNAs into the same blastomere elicits a much stronger ventralizing activity than injection of each into adjacent blastomeres, suggesting that Snh/Bmp7 and Swr/Bmp2b might function through intracellular heterodimer formation.

MATERIALS AND METHODS

Zebrafish *bmp7* homologue isolation

RT-PCR on gastrula stage RNA was performed as previously described (Connors et al., 1999) with the primers CT(G/T)GGNTGGCA(G/A)GACTGGAT and CC(A/G)CA(G/T)-GC(C/T)(C/T)GNACCACCAT. The amplified fragment was used to screen a blastula/gastrula stage zebrafish cDNA library (gift from Thiery Lepage) to isolate a complete *bmp7* cDNA.

Whole-mount in situ hybridization

The *bmp7* coding sequence was subcloned into the *Eco*RI/*Xba*I sites of pBSKII(+). This plasmid was linearized with *Kpn*I and antisense RNA synthesized using T3 RNA-Polymerase. Whole-mount in situ hybridizations were performed as described by Thisse et al. (http://www-igbmc.u-strasbg.fr/zf_info/zfbook/chapt9/9.82.html).

Chromosomal mapping

Mapping was performed as in Nguyen et al. (1998b).

Cloning of *snh*[ty68a]

TÜ wild-type embryos and mutant embryos from a cross of homozygous *snh*[ty68a] fish were collected at bud stage. cDNA was synthesized and PCR performed as in Connors et al. (1999) with the primer pairs 7J-TGTGGACTTCTGCTTAAC and 7G-ATGACCT-TTCTGTTTGCCTC, and 7A-AGCATCAGGAATCCACCTCC and 7D-TCAGAAATCAAGTCAAGTGG to amplify the *bmp7* cDNA. Two independent PCR products were subcloned into pGEM-TEasy (Promega) and sequenced.

mRNA injections

The entire ORF of *bmp7* and *bmp7*[ty68a] was amplified by PCR using the primers 7H-CCGCTTCATATGAAGAAGTC and 7J-TGTGGACTTCTGCTTAACTC, subcloned into pGEM-T and sequenced. We subcloned these inserts into the *Stu*I site of pCS2+. pCS2+bmp7 and pCS2+bmp7[ty68a] were linearized with *Apa*I and mRNA synthesized and injected, as described (Nguyen et al., 1998b).

RESULTS

snailhouse mutant phenotypes

The strongest class of dorsalized mutant defects (C5) identified in large-scale mutagenesis screens in the zebrafish is caused by recessive *swr/bmp2b* mutations and the dominant maternal *somitabun* (*sbn*)/*smad5* mutation (Hild et al., 1999; Mullins et al., 1996; Nguyen et al., 1998b). In mutant embryos of these genes, dorsolateral derivatives are expanded and ventrally encircle the embryo, while ventral cell fates are strongly reduced or absent. The recessive mutation *snh* causes the second strongest class of dorsalized phenotypes (C4). *snh* mutant embryos are morphologically distinguishable as distinctly ovoid shaped embryos just prior to bud stage (Fig. 1A,B). During segmentation stages, the somites extend from their normal dorsal position to ventrolateral regions (Fig. 1D,E). Typically *snh*[ty68a] mutant embryos exhibit a less severe dorsalization than *swr/bmp2b* mutants and display a severe posterior truncation at 1 day post-fertilisation (d.p.f.) with the trunk twisting around its axis in a snail shell-like fashion (Fig. 1G). Occasionally *snh*[ty68a] mutant embryos die around the 14-somite stage, with phenotypes similar to *swr/bmp2b* and *sbn/smad5* mutant embryos.

aubergine (aub) is a dorsalized zebrafish mutant, which arose spontaneously in a wild-type fish stock. This zygotic, recessive mutation gives rise to strongly dorsalized C5 phenotypes, resulting in the extreme elongation (Fig. 1A,C),

Fig. 1. Morphological features of the *snh* mutant. Bud-stage embryos of (A) wild type, (B) *snh*[ty68a] and (C) *snh*[sb1aub] mutants. 7-somite stage (D) wild-type embryo; (E) *snh*[ty68a] mutant embryo (dorsal, posterior view), where the first two somites are laterally enlarged, but do not reach ventral regions, while more posterior somites do. (F) *snh*[sb1aub] mutant (oblique view), where all somites extend to ventral positions. Arrowheads mark the somites in D-F. (G) Same *snh*[ty68a] embryo as in E at 1 d.p.f. (A-D) are lateral views, anterior to the top.

Fig. 2. *snh^{ty68a}* maps to LG11 and is a hypomorphic mutation in the *bmp7* gene. (A) (Left) *snh* maps between markers Z6909 and Z13395 on LG11, 7.3 cM proximal to Z6909. The thick, red bar demarcates the minimal extent of the *Df(LG11)snh^{p11}* and *Df(LG11)snh^{p15}* deletions. (Right) Linkage of marker Z6909 to the *snh^{ty68a}* mutation in single mutant *snh^{ty68a}* embryos, which predominantly show the upper migrating Tü-*snh^{ty68a}*-specific band by PCR amplification. Three recombinants, marked with asterisks, display the Tü-*snh^{ty68a}* and the lower AB*-specific band (top panel). Single sibling embryos show the AB*- and Tü-specific bands or just the lower AB*-specific band. (B) Predicted peptide sequence encoded by the zebrafish *bmp7* gene. Peptide sequence alignment of zebrafish Bmp7 with *Xenopus* Bmp7 (Wang et al., 1997; SPT:Q9YGH), *Xenopus* BMP7R (Nishimatsu et al., 1992; SW:BMP7_XENLA) and mouse BMP7 (Oezkaynak et al., 1990; SW:BMP7_MOUSE). Dashes indicate amino acid identities and dots indicate gaps introduced to optimize the alignment. The predicted signal peptide for secretion is underlined. The arrow points to the valine mutated in *snh^{ty68a}*. The four residues of the maturation cleavage site are boxed and asterisks highlight the seven conserved cysteines. (C) Linkage of *snh^{ty68a}* to the 3′UTR of *bmp7*. An RFLP in the 3′UTR of *bmp7* in the *snh^{ty68a}*/Tü and AB*/AB* founder fish of a mapping cross (lanes 2 and 3). The wild-type chromosome of the *snh^{ty68a}*/Tü fish has the same 3′UTR allele as the AB* line, while the *snh^{ty68a}* chromosome exhibits a polymorphic allele. Pools of homozygous *snh^{ty68a}* (−/−) embryos only show the *snh^{ty68a}*-specific allele (lane 4), while the wild-type siblings display both alleles (lane 5). D) Sequence profile showing the T to G change leading to a valine to glycine transition in the propeptide of Bmp7, causing the *snh^{ty68a}* mutant phenotype. (E) Injection of *bmp7^{ty68a}* and wild-type *bmp7* mRNA into homozygous mutant *snh^{ty68a}* embryos derived from *snh^{ty68a}* homozygous adults. The embryos were grouped into the following phenotypic classes: wild type (wt), C1, C2/C3 and C4/5 (Mullins et al., 1996). All uninjected embryos displayed the strongest C4/5 dorsalized phenotype (red bars). Injection of 50 pg of wild-type *bmp7* mRNA rescues mutants to a wild-type or C1 phenotype (left panel, blue bars), while injection of 50pg of *bmp7^{ty68a}* rescues them much less efficiently (second panel, blue bars). Tenfold higher concentrations of *bmp7^{ty68a}* still rescue much less efficiently than the wild-type construct (third panel). Injection of 60 pg of wild-type *bmp7* mRNA rescues the majority of *snh^{sb1aub}* mutants to a wild-type or C1 phenotype (right panel).
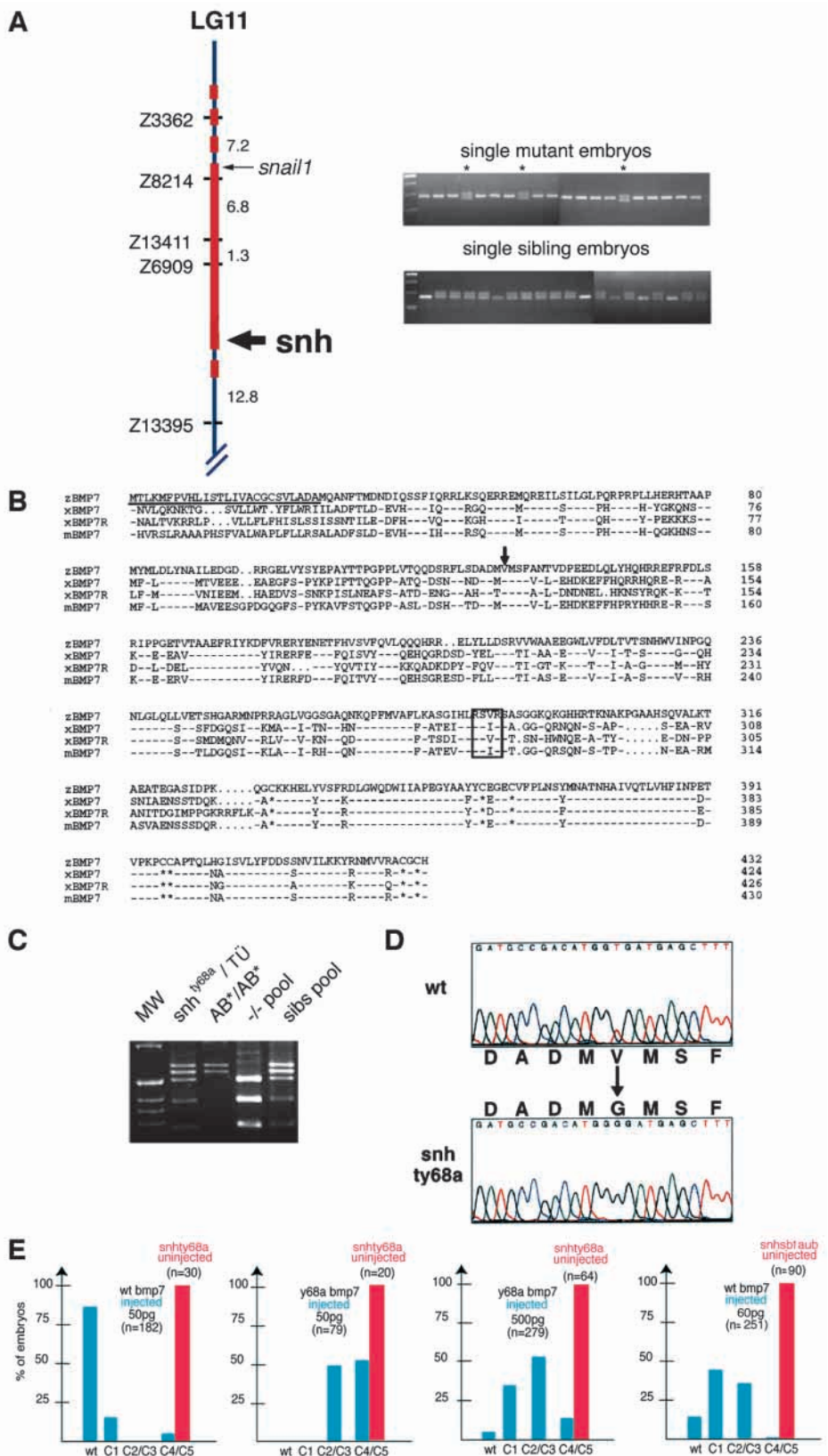
circumferential somites (Fig. 1F) and ultimate death of all mutants by the 15-somite stage. The dorsalization observed in *aub* is more severe than the one typically observed in *snh^ty68a* (Fig. 1E,F) and appears indistinguishable from *swr/bmp2b* mutants. Microinjection of synthetic mRNAs encoding *bmp2b* or *bmp4* (Nikaido et al., 1997) rescues the *aub* mutant phenotype (data not shown), suggesting that this locus encodes a secreted Bmp ligand, rather than a downstream component of the signaling pathway. Sequencing of the *bmp2b* and *bmp4* transcripts from *aub* mutant embryos revealed, however, no mutational alteration.

Since similar conclusions had been reached for *snh* (Nguyen et al., 1998b), we addressed whether *aub* and *snh* are allelic to each other. In crosses between heterozygous fish of these two mutations, *aub* failed to complement *snh^ty68a* in six independent crosses (22% of the embryos showed a C4 or C5 phenotype, 172/620). We therefore consider *aub* a stronger allele of *snh* (as further confirmed by mapping data below) and rename it *snh^sb1aub*.

snailhouse maps to LG11 and is syntenic to *bmp7* in the mouse

To identify potential candidate genes for the *snh* mutations, we mapped *snh* to a chromosomal location using SSLP markers (Knapik et al., 1998). In pools of mutant and sibling embryos in the F$_2$ generation of a mapping cross, we found that the SSLP marker Z6909 on LG11 was linked to the *snh* mutation (Fig. 2A). In analyzing 150 *snh^ty68a* chromosomes, we identified 11 recombinants, placing *snh^ty68a* 7.3 cM from marker Z6909 (Fig. 2A). Examination of three additional SSLP markers shows that *snh* is located proximal to Z6909 on LG11 (data not shown). In our *snh^sb1aub* line, we found SSLP marker Z13395 on LG11, located 13 cM proximal to marker Z6909 (Fig. 2A), to be 6 cM (5 recombinants in 84 meioses) from the *snh^sb1aub* mutation. Analysis of an additional marker distal to Z6909 places the *snh^sb1aub* mutation at the same position as *snh^ty68a*, consistent with these mutations being allelic to each other.

In zebrafish, the *snail1* gene also maps to LG11 (Postlethwait et al., 1998) and we found it to be approximately 16 cM telomeric to the *snh^ty68a* mutation (Fig. 2A, data not shown). Since we previously observed that *snh^ty68a* mutant embryos are most efficiently rescued by *Xbmp7* overexpression, as opposed to *bmp2b* and *bmp4* (Nguyen et al., 1998b), we examined the possibility of conserved chromosomal synteny between the *snail1* gene and the *bmp5,6,7* subclass of Bmps in the mouse and human. Interestingly, the mouse *bmp7* gene maps 5 cM from the *snail* homologue (www.informatics.jax.org/searches/quick_gene_report). Given the previously observed conserved synteny between mouse, human and zebrafish species (Postlethwait et al., 1998) and our previous rescue results, we reasoned that *bmp7* was an excellent candidate for the *snh* gene.

Isolation of a zebrafish *bmp7* homologue

By RT-PCR with degenerate primers and cDNA library screening we isolated a zebrafish *bmp7* cDNA. The encoded protein belongs to the BMP7/OP1 subgroup of TGFβs and is most closely related to *Xenopus* XBMP7 (67.8% identical; 75.1% similar amino acids), and mouse BMP7/OP1 (66.2% identity; 73.9% similarity), but is slightly less related to
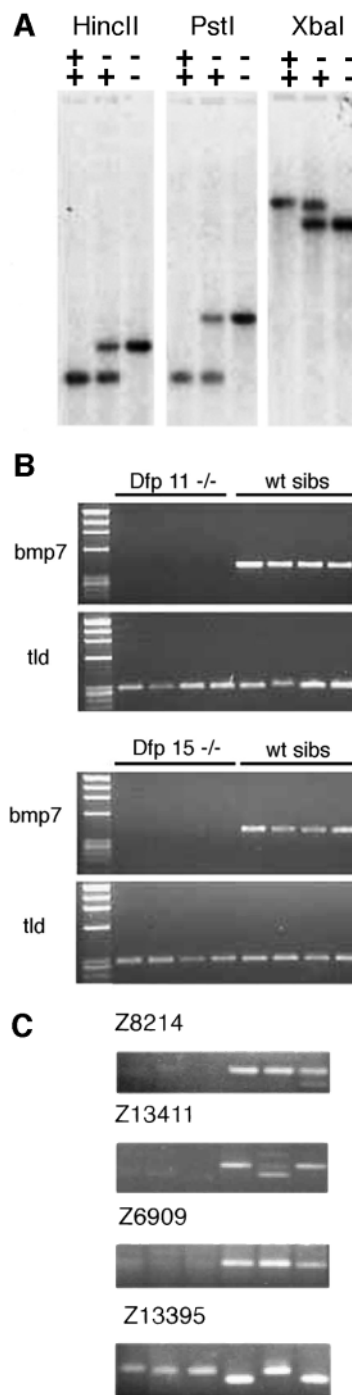
Fig. 3. The *bmp7* gene in *snh^sb1aub*, *Df(LG11)snh^p11* and *Df(LG11)snh^p15* alleles. (A) DNA of wild-type (+/+), heterozygous (+/−), and homozygous (−/−)*snh^sb1aub* genotypes was digested and analyzed by genomic Southern blot, probed with the *bmp7* 3′UTR. This shows that the *snh^sb1aub* chromosome is associated with an alteration of the *bmp7* locus. (B) No *bmp7* 3′UTR PCR amplification product is observed in homozygous *Df(LG11)snh^p11* (Dfp11) and *Df(LG11)snh^p15* (Dfp15) mutant embryos, while it is amplified from wild-type sibling DNA. The bottom panels show an amplification product for the *tolloid* (tld) gene, confirming the integrity of the DNA. (C) The markers Z8214, Z13411 and Z6909 were absent in *Df(LG11)snh^p11* and *Df(LG11)snh^p15* homozygous mutants (lanes 1-3 of each gel), while they were present in wild-type siblings (lanes 4-6). Marker Z13395 was present in DNA of mutant and wild-type siblings.

Xenopus XBMP7R (57.2% identity; 64.8% similarity) (Fig. 2B). A predicted 26-amino-acid signal peptide for secretion is followed by a 261-amino-acid prodomain and a conserved BMP maturation cleavage site (RSVR) (Fig. 2B). The 145 C-terminal amino acids of the presumptive mature Bmp7 peptide contain the seven invariant cysteine residues necessary for dimerization and formation of the characteristic TGFβ cysteine-knot structure.

snailhouse is a mutation in *bmp7*

To investigate whether the *bmp7* gene corresponds to *snh*, we examined linkage of *bmp7* to the *snh* mutation. We identified an RFLP in the 3′UTR of *bmp7* in a *snh^ty68a* mapping cross line and followed the segregation of the RFLP in individual F₂ mutant and wild-type sibling embryos (Fig. 2C). In 162 meioses we always observed segregation of the polymorphism with the mutation (data not shown), placing the *snh^ty68a* mutation within 0.6 cM of the *bmp7* gene.

To determine if a mutation in the *bmp7* gene causes the *snh* mutant phenotype, we cloned the *bmp7* cDNA from *snh^ty68a* mutant embryos. The sequence of the *snh^ty68a* allele revealed a missense mutation in the prodomain, changing valine 130 to a glycine residue (Fig. 2D). To confirm that this mutation is the cause of the *snh^ty68a* phenotype, we assayed the ability of the mutant *bmp7* allele (*bmp7^ty68a*) to rescue the *snh^ty68a* phenotype. We injected 50 pg of *bmp7^ty68a* mRNA into *snh^ty68a* mutant embryos derived from homozygous adult parents (previously rescued to viable adults, as described in Nguyen et al., 1998b) and observed only partial rescue of the mutants to a slightly weaker phenotype (Fig. 2E). In contrast, 50 pg of the wild-type *bmp7* allele rescues 99% of the *snh^ty68a* mutant embryos to a wild-type or very weakly dorsalized (C1) phenotype (Fig. 2E). At tenfold higher concentrations (500 pg), however, *bmp7^ty68a* mRNA can rescue *snh^ty68a* mutants to less severely dorsalized phenotypes and occasionally to a wild-type phenotype (Fig. 2E). This demonstrates that the valine residue at position 130 in the Bmp7 protein is essential for its proper function, although the mutant protein still displays some weak activity. This mutation may affect the stability, secretion or maturation of the ligand.

Absence of *bmp7* transcript suggests that *snh^sb1aub* is a *bmp7* null mutant

We next pursued the identification of the defect responsible for the stronger *snh^sb1aub* allele. Attempts to amplify the *bmp7* cDNA from *snh^sb1aub* mutant embryos by RT-PCR, however, repeatedly failed, despite our ability to isolate both *bmp2b* and *bmp4* from *snh^sb1aub* mutants (data not shown). Moreover, no *bmp7* expression is detectable by in situ hybridization in *snh^sb1aub* mutant embryos at any stage of development examined, in contrast to the equally severely dorsalized *swr/bmp2b* mutant (see below; Fig. 5L,O; data not shown). Thus, no *bmp7* transcripts are detectable in *snh^sb1aub* mutants, indicating that *snh^sb1aub* represents a null mutation of the *bmp7* gene.

We show by Southern blot analysis probing with the 3′UTR fragment of the *bmp7* cDNA that the *bmp7* locus is altered in the *snh^sb1aub* mutant. With all restriction enzymes tested, we observed two different size restriction fragments for homozygous mutant and homozygous wild-type DNA, and the presence of both bands from DNA of heterozygous fish (Fig.

3A). Considering the altered genomic structure of this gene, it is possible that the absence of the *bmp7* transcript in *snh^sb1aub* mutant embryos is due to an insertion or local genomic rearrangement.

We investigated whether *snh^sb1aub* mutants could be rescued to homozygous adults, as we had previously found with the hypomorph *snh^ty68a* (Nguyen et al., 1998b). Indeed, injection of 60 pg of *bmp7/snh* mRNA rescues a substantial fraction of the mutants to a wild-type or very weakly dorsalized phenotype (60%, Fig. 2E). Furthermore, we could raise the majority of rescued *snh^sb1aub* homozygotes to viable, fertile adults. Like *snh^ty68a*, *snh^sb1aub* homozygous females do not exhibit a maternal-effect mutant phenotype, indicating no significant maternal contribution of Bmp7/Snh to embryonic development. These results together with the non-complementation and mapping data confirm that the dorsalized phenotype of *snh^sb1aub* is due to the specific loss of Bmp7 activity.

Generation of *bmp7* deficiencies

Since the *snh^ty68a* allele is a hypomorph, and the precise molecular lesion responsible for the potential null allele *snh^sb1aub* is not completely characterized, we undertook the isolation of gamma ray-induced deficiencies of *snh/bmp7*. Gamma rays typically cause deletions and translocations (Fritz et al., 1996), which can be valuable in analyzing the null phenotype of a gene. We performed a non-complementation screen between homozygous *snh^ty68a* females and males generated from gamma-ray irradiated sperm. We screened 205 males and identified two males that failed to complement the *snh/bmp7* mutation to generate the lines, *Df(LG11)snh^p11* and *Df(LG11)snh^p15*. Similar to other gamma ray-induced mutations, the *Df(LG11)snh^p11* and *Df(LG11)snh^p15* mutations did not segregate in a Mendelian manner. Crosses between homozygous *snh^ty68a* females and *Df(LG11)snh^p11* or *Df(LG11)snh^p15* males produced 1-25% mutant embryos, instead of the 50% expected. Intercrosses of the *Df(LG11)snh^p11* and *Df(LG11)snh^p15* lines generated broods with 1-12% mutant embryos.

To determine if the *bmp7* gene was deleted, we performed PCR with *bmp7*-specific primers on DNA from *Df(LG11)snh^p11* and *Df(LG11)snh^p15* mutant embryos. Mutant DNA never yielded a 3′UTR PCR amplification product of *bmp7*, whereas wild-type sibling DNA always did (Fig. 3B). Primers specific to *tolloid* served as a positive control for the quality of the mutant DNA (Fig. 3B). Thus, the *bmp7* 3′UTR is deleted in both lines.

To determine the extent of the deletions we examined SSLP markers surrounding the *bmp7* locus. The markers Z8214, Z13411 and Z6909 distal to *snh/bmp7* failed to produce a PCR amplification product from mutant DNA, whereas sibling DNA did (Fig. 3C). We amplified the next proximal marker to *snh*, Z13395, from mutant DNA, indicating that the deficiency does not extend beyond this marker (Fig. 3C). Thus, the deficiency includes the region from *snh/bmp7* to at least marker Z8214, encompassing a minimum of 15.4 cM (Fig. 2A).

Expression of *bmp7* during embryogenesis

We next studied the embryonic expression of *bmp7* to investigate whether its expression domains are compatible with a proposed role in the early specification of ventral cell fates.
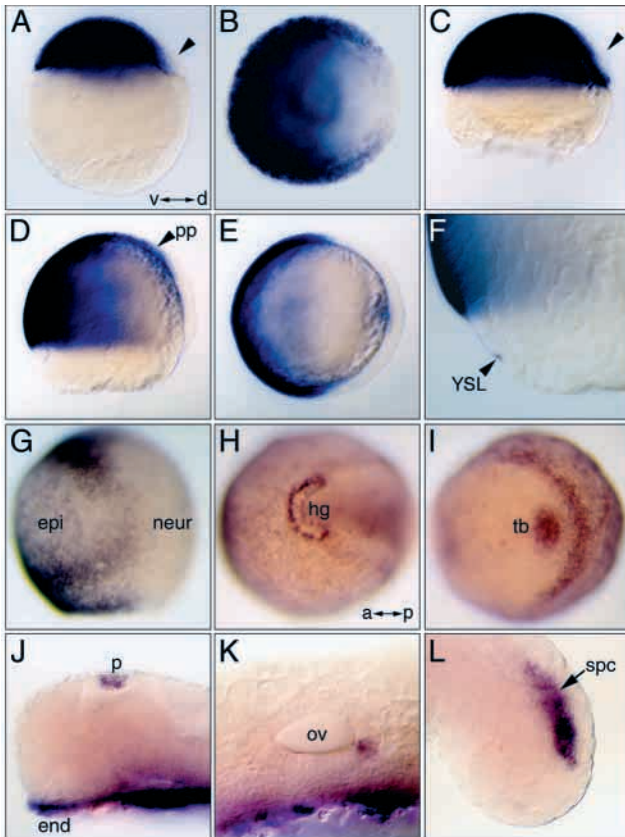
Fig. 4. *bmp7* expression during embryogenesis. (A) 30% epiboly
stage (lateral view). Expression extends throughout the blastoderm,
except its dorsal marginal aspect (arrowhead). Animal pole (B) and
lateral (C) views of a germ ring stage embryo showing *bmp7*
downregulation in the dorsal quadrant. (D-F) 60% epiboly stage.
Lateral (D) and transverse optical cross-sectional (E) views showing
expression throughout the ventral gastrula and in the prechordal plate
(pp) (D). (F) Close-up of the ventral margin showing expression in
the YSL. (G) Lateral view at 90% epiboly. Robust expression is seen
at the border between epidermal (epi) and neurogenic (neur)
ectoderm and in the ventral margin. Faint expression is observed
throughout the epidermal territory. (H,I) 3-somite stage. (H) Dorsal
cephalic view. Transcripts accumulate at the border of the hatching
gland (hg). Faint expression is detected outside the neural plate.
(I) Posterior view. Transcripts are localized to the tail bud (tb) and
the border between neural and non-neural posterior ectoderm.
At 24 h.p.f. expression is observed in (J) the endoderm (end) and the
pineal gland (p), (K) the posterior aspect of the otic vesicle (ov) and
(L) dorsal posterior neural tissue (spc) of the tail. A-G, dorsal to the
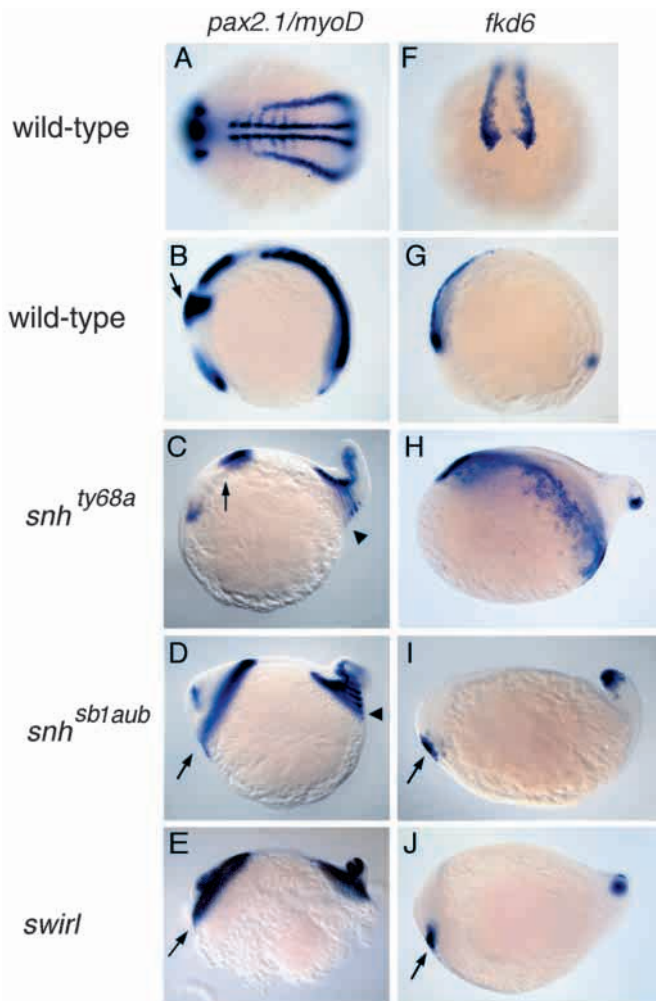right; H-K, anterior to the left.

Both in situ hybridization and RT-PCR failed to detect any
maternally deposited *bmp7* RNA (data not shown), consistent
with the lack of a maternal-effect phenotype of homozygous
snh females. *bmp7* expression first becomes detectable
uniformly throughout the blastoderm shortly after the
activation of the zygotic genome (data not shown). At 30%
epiboly, transcripts start to be excluded from the presumptive
dorsalmost region of the embryo (Fig. 4A) and this restriction
of *bmp7* expression to ventrolateral regions becomes more
pronounced at the beginning of gastrulation (Fig. 4B,C). At
60% epiboly, *bmp7* is expressed in the ventral half of the
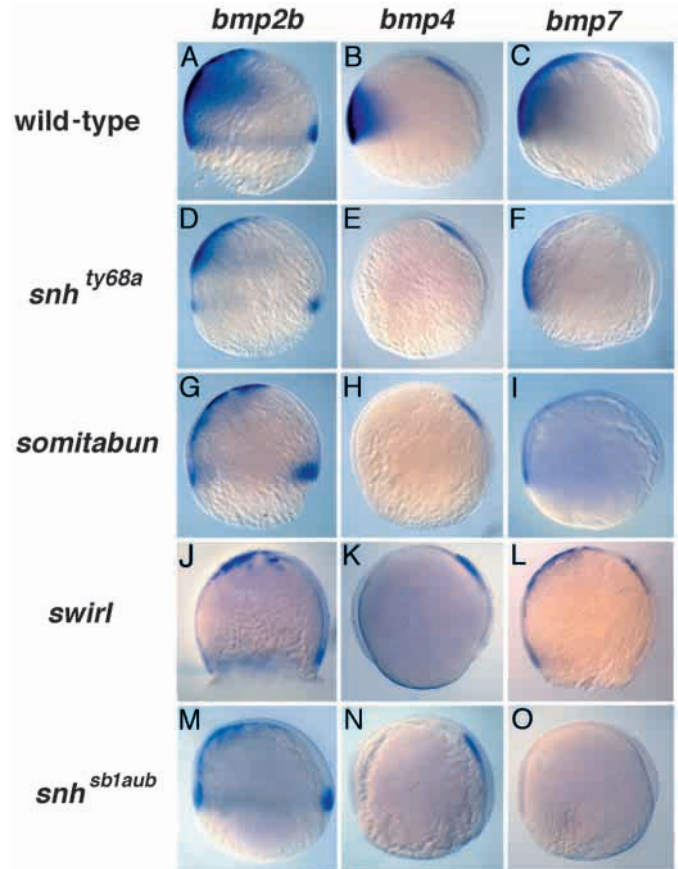
Fig. 5. Expression of *bmp2, 4* and *7* in dorsalized mutant embryos at
65-75% epiboly. Expression in wild-type embryos of *bmp2b* (A),
bmp4 (B), and *bmp7* (C). Expression of *bmp2b*, *bmp4* and *bmp7* in
mutant embryos of *snh^{ty68a}* (D-F), *sbn^{dtc24}* (G-I), *swr^{ta72}/bmp 2b* (J-
L) and *snh^{sb1aub}* (M-O), respectively. In *snh^{ty68a}* mutants *bmp2b* (D)
and *bmp7* (F) expression are reduced in amount and to a more ventral
domain. *bmp4* expression is absent in *snh^{ty68a}*(E), *sbn* (H), *swr* (K)
and *snh^{sb1aub}* (N) on the ventral side, whereas the dorsal expression
domain is unaffected. *bmp2b* expression is absent in the hypoblast
ventrally, but is still present in the YSL and the dorsal margin in
sbn/smad5 (G), *swr/bmp2b* (J) and *snh^{sb1aub}* (M) mutant embryos.
bmp7 expression is reduced in *sbn/smad5* (I) and absent in
swr/bmp2b mutant embryos, except for expression in the YSL and
prechordal plate (L). In *snh^{sb1aub}* mutants there is no detectable *bmp7*
expression, including the YSL and prechordal plate expression
domains (O).

gastrula (Fig. 4D,E), as well as in the yolk syncytial layer
(YSL) (Fig. 4F) and weakly in the prechordal plate (Fig. 4D).
The expression of *bmp7* in the ventral blastula and gastrula
stage embryo supports a role for this factor in the early
specification of ventral cell fates. At late gastrulation stages
(Fig. 4G), expression delineates the boundary of the anterior
neural plate, while weak expression is observed throughout the
non-neural ectoderm. Moreover, transcripts are detected in the
ventral marginal zone (data not shown).

At early segmentation stages, transcripts have vanished from
the border of the anterior neural plate, while very weak
expression is still observed outside the neurogenic ectoderm
(Fig. 4H). At this time, expression is observed at the border of
the hatching gland (Fig. 4H), as well as posteriorly in the tail

pax2.1/myoD   fkd6

wild-type

wild-type

snh^ty68a

snh^sb1aub

swirl

Fig. 6. In situ hybridizations with *pax2.1* and *myoD* (A-E) and *fkd6* (F-J) in wild-type, *snh/bmp7* and *swr^ta72/bmp2b* mutant embryos at the 5-somite stage. Lateral views, anterior to the left, except (A,F). (A) The somitic expression of *myoD* and the pronephric expression of *pax2.1* in a dorsal-posterior view of a wild-type embryo. (B) The midbrain/hindbrain boundary (MHB) expression of *pax2.1* (arrow) in a wild-type embryo. (C) *snh^ty68a* displays a slight lateral expansion of the MHB (arrow), not visible in this lateral view. The somites posterior to somite 2 encircle the embryo (arrowhead). (D) In *snh^sb1aub* mutant embryos the MHB (arrow) and all somites (arrowhead) encircle the embryo. (E) Homozygous *swr^ta72* mutants are indistinguishable from *snh^sb1aub* mutants. *fkd6* expression in the cranial neural crest progenitors in wild-type in an anterior (F) (dorsal to the top) and lateral (G) view. *fkd6* expression is also observed in the tail bud (G). (H) Expanded cranial neural crest expression in *snh^ty68a*. In *snh^sb1aub* (I) and *swr/bmp2b* (J) mutants, the number of cranial neural crest progenitors is severely reduced (arrow).

bud and at the border between neural and non-neural posterior ectoderm (Fig. 4I). At later somitogenesis stages, *bmp7* begins to be expressed in the epiphysis, where it persists until late stages of embryogenesis (Fig. 4J). At 24 hours (h.)p.f., *bmp7* transcripts are detectable in the posterior aspect of the otic vesicle (Fig. 4K). Further expression domains include the endoderm (Fig. 4J,K) and posterior dorsal neural tissue (Fig. 4L). At 48 hpf, additional expression is observed in a subset
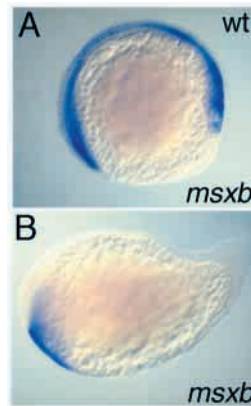
Fig. 7. Expression of *msxB* in *swr/bmp2b; snh/bmp7* double mutant embryos. Expression of *msxB* in 5-somite stage (A) wild-type and (B) mutant embryos of crosses between *swr^tc300a/+*; *snh^sb1aub/+* double heterozygous fish.

of cells in the hyoid arch as well as ectodermal cells surrounding the mouth opening (data not shown).

Regulation of *bmp7* expression in dorsalized mutants

We previously showed that expression of the *bmp2b* and *bmp4* genes is initiated in *swr/bmp2b*, *sbn/smad5* and *snh^ty68a/bmp7* mutant embryos, while maintenance of *bmp2b* and *bmp4* expression is affected (Nguyen et al., 1998b). To test if *bmp7* gene expression is also altered in these mutants, we examined expression of *bmp7* by in situ hybridization. At sphere stage and 50% epiboly, just prior to gastrulation, *bmp7* expression in *snh^ty68a*, *sbn/smad5*, and *swr/bmp2b* mutants is indistinguishable from wild-type embryos (data not shown). After the onset of gastrulation, the expression of *bmp7* becomes downregulated in these mutants (Fig. 5C,F,I,L), similar to that observed with *bmp2b* and *bmp4* expression (Fig. 5A,B,D,E,G,H,J,K). In *snh^ty68a* and *sbn/smad5* mutant embryos, *bmp7* expression becomes restricted to a more ventral domain (Fig. 5F,I). However, in midgastrula-stage *swr/bmp2b* mutant embryos, *bmp7* expression is absent from the ventral blastoderm, while it is still detectable in the prechordal plate and the ventral YSL (Fig. 5L). Thus, the initiation of *bmp7* expression is not perturbed in *swr/bmp2b*, *sbn/smad5* and *snh/bmp7* mutant embryos, while maintenance of *bmp7* expression is affected.

In *snh^sb1aub* mutants, a lack of ventral embryonic *bmp2b* and *bmp4* expression at gastrulation stages is observed similar to that in *swr/bmp2b* mutants (Fig. 5J,M and K,N). In contrast, we did not detect *bmp7* expression at any stage examined in *snh^sb1aub*, *Df(LG11)snh^p11* and *Df(LG11)snh^p15* mutant embryos (Fig. 5O, data not shown). In these mutant embryos, unlike *swr/bmp2b* mutants, *bmp7* expression is also absent from the YSL and the prechordal plate (Fig. 5, compare L to O, data not shown). Thus, the absence of all *bmp7* expression domains in *snh^sb1aub*, *Df(LG11)snh^p11* and *Df(LG11)snh^p15* mutant embryos is consistent with these mutations being null alleles for *bmp7*.

Null alleles of *snh/bmp7* are indistinguishable from *swr/bmp2b*

To characterize and compare the phenotypic strengths of *snh^ty68a*, *snh^sb1aub*, and deletions *Df(LG11)snh^p11* and *Df(LG11)snh^p15* to the strongest dorsalized mutant, *swr/bmp2b*, we examined the expression of several markers that distinguish between strong and moderately strong dorsalized phenotypes. We previously showed that all somites of *swr/bmp2b* mutant embryos encircle the embryo, whereas in *snh^ty68a* only somites posterior to somite 2 typically circle the embryo (Fig. 1E; Mullins et al., 1996). We examined the expression of *myoD* (Weinberg et al.,

1996), a somitic mesodermal marker, and found that in both snh^{sb1aub} and $Df(LG11)snh^{p15}$ mutants all the somites form rings around the embryo, identical to the $swr/bmp2b$ mutant phenotype (Fig. 6A,C-E). We found all aspects of the $Df(LG11)snh^{p15}$ mutant embryos indistinguishable from snh^{sb1aub} and therefore only show snh^{sb1aub} here. In examining the expression of $pax2.1$ (Krauss et al., 1991), we observed the midbrain-hindbrain boundary domain to encircle the entire embryo in $Df(LG11)snh^{p15}$, snh^{sb1aub} and $swr/bmp2b$ fish, whereas in snh^{ty68a} embryos it is enlarged laterally, but never encircles the embryo (Fig. 6B-E; Mullins et al., 1996). Thus, a stronger dorsalized phenotype is displayed in the deficiency and snh^{sb1aub} embryos than in snh^{ty68a} mutants.

We previously found that specification of the cranial neural crest is very sensitive to variations in Bmp activity. In mutants with presumptive low Bmp signaling activity, cranial neural crest progenitors are expanded, while in mutants with no or very low Bmp signaling activity, cranial neural crest is greatly reduced to absent (Nguyen et al., 1998b). In snh^{ty68a} the presumptive cranial neural crest, as revealed by $fkd6$ expression (Odenthal and Nüsslein-Volhard, 1998), is expanded (Fig. 6F-H), consistent with the hypomorphic nature of the snh^{ty68a} allele and the presence of residual Bmp activity. In contrast, $swr/bmp2b$, snh^{sb1aub} and $Df(LG11)snh^{p15}$ mutant embryos display little or no $fkd6$-expressing neural crest progenitors (Fig. 6I,J).

Consistent with snh^{ty68a} exhibiting a weaker phenotype morphologically and $bmp7^{ty68a}$ mRNA overexpression providing some weak rescuing activity, our marker analysis also indicates the presence of residual Bmp7 activity in snh^{ty68a} mutant embryos. Furthermore, the identical phenotypic strengths of $Df(LG11)snh^{p11}$ and $Df(LG11)snh^{p15}$ to snh^{sb1aub} mutant embryos strongly supports our hypothesis that snh^{sb1aub} is a null allele of $bmp7$. The strength of the dorsalization displayed by snh^{sb1aub} embryos appears equivalent to that of $swr/bmp2b$ mutants, indicating that Bmp activity is reduced to the same degree in complete loss of function alleles of $snh/bmp7$ and presumptive null alleles of $swr/bmp2b$.

$swr/bmp2b$; $snh/bmp7$ double mutants do not display a stronger phenotype than single mutants

We investigated whether $swr/bmp2b$ and $snh/bmp7$ display redundant functions in early embryonic development, by examining swr; snh double mutant embryos. Embryos from intercrosses of double heterozygous $swr^{tc300a}/+$, $snh^{sb1aub}/+$ fish did not display any detectable morphological alterations distinct from the single mutants (data not shown). We also analyzed $msxB$ expression, a marker of dorsal neuroectodermal tissue during segmentation stages (Ekker et al., 1997) which, similar to neural crest markers (Nguyen et al., 1998b), is very sensitive to variations in the amount of Bmp signaling (V. H. Nguyen and M. C. M., unpublished). In $swr/bmp2b$ and $snh/bmp7$ mutants, we observe residual $msxB$ expression (Fig. 7A,B), which could reflect redundant Bmp7/Snh signaling still present in $swr/bmp2b$ mutants. In mutant embryos from crosses between double heterozygous swr^{tc300a}, snh^{sb1aub} fish, however, we never observed a strong reduction or absence of $msxB$ expression, which would be expected if the double mutants display reduced Bmp signaling activity compared to the single mutants (Fig. 7B, 855 total embryos examined). The

lack of additional phenotypes or a stronger dorsalization in double mutant embryos suggests that $bmp2b$ and $bmp7$ do not function redundantly during early development in the zebrafish.

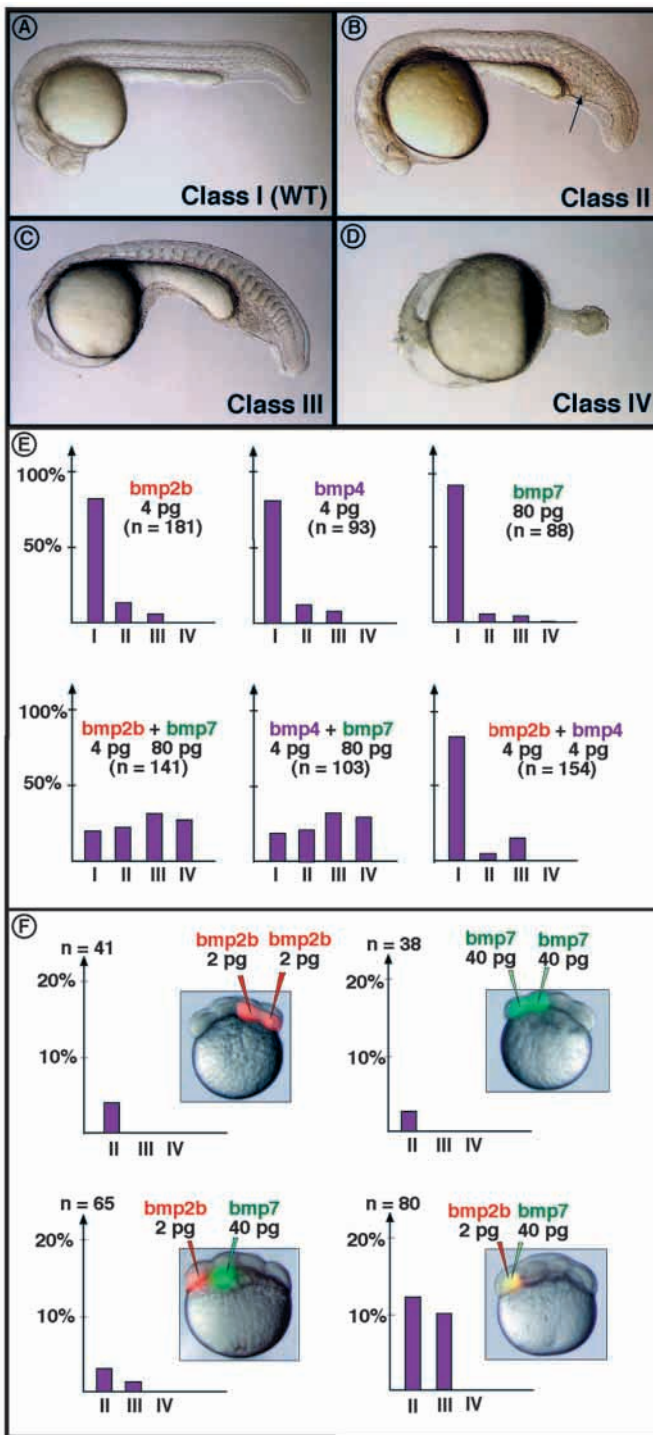### $bmp2b$ and $bmp7$ synergize in overexpression experiments

To investigate the combined versus single activities of $bmp2b$ and $bmp7$, we injected mRNA for $bmp2b$ or $bmp7$ either separately or in combination into the yolk of 2-cell stage wild-type zebrafish embryos. The resulting embryos were scored according to their morphology. Class I embryos display a wild-type morphology (Fig. 8A). Weakly ventralized class II embryos show a slight reduction of the head and an expansion of ventroposterior hematopoietic derivatives (Fig. 8B). Class III embryos lack all dorso-axial derivatives, including the head and notochord (Fig. 8C). The most severely affected class IV embryos acquire a spindle shape devoid of morphologically identifiable dorsoventral polarity and contain a large quantity of blood cells at their posterior extremity (Fig. 8D).

Both $bmp2b$ and $bmp7$ can induce severely ventralized class III/IV phenotypes if overexpressed at sufficiently high doses (20 pg and 400 pg of mRNA, respectively; data not shown). Coinjection of both mRNAs, however, leads to a clear synergistic increase in ventralizing potency. Following the separate injection of 4 pg $bmp2b$ or 80 pg $bmp7$ RNA, over 80% of the embryos still display a wild-type morphology (Fig. 8E). In contrast, the combined injection of these same doses of $bmp2b$ and $bmp7$ mRNA leads to a substantial decrease in wild-type embryos (to 19.8%) and a concomitant increase in strongly ventralized class III/IV phenotypes (to 58.2%). The coinjection of 4 pg $bmp2b$ with 80 pg $bmp7$ mRNA has the same effect as separate injections of either 20 pg $bmp2b$ or 400 pg $bmp7$ mRNA, suggesting that the combined presence of both factors increases their ventralizing potency.

We next addressed whether the synergy observed in our coinjection experiments was specific to $bmp2b$ and $bmp7$ or whether similar effects could be obtained by any two of the gastrula-expressed $bmps$: $bmp2b$, $bmp4$ and $bmp7$. We expressed combinations of $bmp2b$, $bmp4$ or $bmp7$, any one of which had only a very weak ventralizing effect (Fig. 8E). In combinations, however, we observed that the ventralizing potency of either $bmp2b$ or $bmp4$ was strongly enhanced by coexpression of $bmp7$, while in contrast no synergistic interaction was detectable between $bmp2b$ and $bmp4$ (Fig. 8E).

Bmp2b and Bmp7 may activate different receptors, which synergize at a downstream level. Alternatively, the cooperation between Bmp2b and Bmp7 could be mediated through more active heterodimers of these factors. In this case, synergy would depend on the coexpression of $bmp2b$ and $bmp7$ in the same cell, since Bmp dimers form intracellularly. To test whether the synergistic effect could be mediated through the non-cell-autonomous interaction of Bmp2b and Bmp7, mRNAs encoding $bmp2b$ or $bmp7$ together with two different fluorescent dyes were injected either separately into two neighboring blastomeres or coinjected into the same cell of 16-cell stage embryos (Fig. 8F). Observation of the clonal derivatives of the injected

Fig. 8. Bmp2b and Bmp7 interact synergistically in a cell-autonomous manner. (A-D) Lateral views of live 24 h.p.f. embryos of the four phenotypic classes resulting from injection of *bmp* mRNAs. (A) Class I embryos display wild-type morphology. (B) In class II embryos the head is slightly reduced, while the hematopoietic mesoderm is expanded (arrow). (C) Class III embryos lack head and notochord. (D) Class IV embryos acquire a spindle shape lacking obvious dorsoventral polarity. (E) Phenotypic distributions following the expression of different *bmps* either separately or in combination. A synergistic increase in ventralizing potential is observed following the coexpression of *bmp2b* or *bmp4* with *bmp7*, but not following the coexpression of *bmp2b* with *bmp4*. (F) Separate injection of one dose of *bmp2b* RNA and one dose of *bmp7* RNA in adjacent blastomeres (lower, left panel) does not cause an enhanced effect compared to the injection of two doses of *bmp2b* or *bmp7* (upper panels). A cooperative effect between *bmp2b* and *bmp7* is only observed if RNAs for both factors are coinjected in the same cell (lower, right panel).

DISCUSSION

Bmp7 and Bmp2b mediate equivalent, non-redundant genetic functions in dorsoventral patterning

The strongest dorsalized phenotype isolated during zebrafish mutagenesis screens is associated with the loss of *swr/bmp2b* gene function. We previously showed that embryos homozygous for the *snh^{ty68a}* mutation display a comparatively weaker dorsalization (Mullins et al., 1996; Nguyen et al., 1998b). In this study, we report that *snh^{ty68a}* is a hypomorphic mutation in the zebrafish *bmp7* gene. Furthermore, we show that null mutations of *snh/bmp7* cause a more severe dorsalization, indistinguishable from the one observed in *swr/bmp2b* mutant embryos, and *swr/bmp2b; snh/bmp7* double mutant embryos display a phenotype identical to that of the single mutants. Therefore, Bmp7 and Bmp2b mediate equivalent, non-redundant, ventralizing activities required for dorsoventral pattern formation of the zebrafish embryo.

Bmp signaling in early vertebrate embryos

In the mouse it has been difficult to address the roles played by various Bmps during gastrulation. Most Bmp4 and all Bmp type I receptor mouse mutants die prior to gastrulation, precluding an analysis of their roles in dorsoventral pattern formation (Mishina et al., 1995; Winnier et al., 1995). A small fraction of *bmp4* mutant embryos that survive beyond this stage exhibit defects in ventroposterior tissue consistent with a role in dorsoventral patterning. The lack of gastrulation defects in *bmp5*, *bmp6* and *bmp7* mouse mutants or *bmp5; bmp7* and *bmp5; bmp6* double mutants may reflect possible maternal or redundant expression of these or other *bmp* genes, as shown for other tissues in the mouse (Solloway et al., 1998; Solloway and Robertson, 1999; Storm and Kingsley, 1996).

In *Xenopus bmp2, 4* and *7* behave similarly in many misexpression and explant assays tested. Overexpression of cleavage-defective dominant-negative *bmp2, 4* or *7* mutants similarly dorsalize the embryo (Hawley et al., 1995; Suzuki et al., 1997b). Although caveats exist in the interpretation of results generated from dominant-negative mutants, the data are consistent with a requirement for multiple Bmps in dorsoventral patterning, similar to our results in the zebrafish.

blastomeres at early gastrula stages revealed extensive intermingling between *bmp2b*- and *bmp7*-expressing cells (data not shown). We found that the percentage of ventralized embryos is clearly enhanced, if both mRNAs are injected into the same blastomere as opposed to separate injections into adjacent cells (Fig. 8F). The cooperation between *bmp2b* and *bmp7* is therefore mediated through a cell-autonomous mechanism, suggesting that these two factors cooperate to specify ventral embryonic fates through heterodimer formation.

Bmp signaling in the fish versus the fly

While arthropods and vertebrates display an inverted body plan with respect to the dorsoventral axis, certain aspects of dorsoventral patterning have been conserved (De Robertis and Sasai, 1996; Ferguson, 1996), while other aspects appear divergent. As in the zebrafish, two TGFβ family members in the fly, *dpp* and *screw*, are required for specification of dorsal cell fates. While *dpp* is the *Drosophila* orthologue of *bmp2/bmp4*, *screw* is a distant relative of the *bmp5,6,7* subclass, with no clear vertebrate orthologue (Arora et al., 1994). Null mutations of *dpp* eliminate all dorsal structures, while *screw* null mutants lack only a subset of these derivatives, revealing the non-equivalent roles of these genes, unlike the equivalent genetic roles for *bmp2b/swr* and *bmp7/snh* in the zebrafish. Moreover, *dpp* and *screw* exhibit different rescuing activities in overexpression experiments and can interact non-cell autonomously through the stimulation of different receptors (Arora et al., 1994; Neul and Ferguson, 1998; Nguyen et al., 1998a). We show that the ventralizing synergy between *bmp2b* and *bmp7* depends on their cell-autonomous expression. Therefore, while the fly and the zebrafish both depend on two different Bmps for dorsoventral patterning, the respective roles of these genes differ in the two organisms.

Requirement of *bmp2b* and *bmp7* in early patterning in the zebrafish

The failure of either *bmp7* or *bmp2b* to ensure proper specification of ventral fates alone, together with the similar expression, activities and mutant phenotypes of these genes, suggests that these two factors may cooperate to achieve proper embryonic patterning. This is further supported by our finding that coexpression of *bmp7* and *bmp2b* strongly enhances the ventralizing potential of either *bmp* alone. Several mechanisms by which such cooperation could be achieved are discussed below.

According to a first model, Bmp2b and Bmp7 could simply have additive, dosage effects. This mechanism may depend on a positive transcriptional autoregulatory loop, in agreement with the observed downregulation of *bmp2b*, *4* and *7* expression in *swr/bmp2b*, *snh/bmp7* and *sbn/smad5* mutant embryos. Insufficient Bmp signaling in the mutants could account for the disruption of a transcriptional autoregulatory loop (Kim et al., 1998; Metz et al., 1998). However, such a model would predict a strong effect following the simultaneous loss of one copy of *bmp2b* and one copy of *bmp7*. The lack of consistent severely dorsalized phenotypes in *snh/bmp7; swr/bmp2b* double heterozygotes (data not shown), therefore, argues against this mechanism as being the sole one for Bmp2b and Bmp7 in dorsoventral patterning.

Other possible mechanisms involve the specific requirement of either Bmp2b and Bmp7 homodimers or Bmp2b/Bmp7 heterodimers. Bmp2b and Bmp7 homodimers may independently stimulate distinct receptors required for the activation of downstream components, or both may be required for the stimulation of the same receptor tetramer, as has been suggested for Dpp and Screw in *Drosophila* (Neul and Ferguson, 1998; Nguyen et al., 1998a). Alternatively, Bmp2b and Bmp7 may interact by formation of heterodimers that are required for receptor activation. In several experimental systems, Bmp heterodimers display increased potency compared to homodimers (Aono et al., 1995; Israel et al., 1996; Nishimatsu and Thomsen, 1998; Suzuki et al., 1997a). Furthermore, an endogenous role for Bmp heterodimers has been suggested from the analysis of an antimorphic mutation in the human Bmp family member CDMP1 (Thomas et al., 1997). Thus, Bmp2b and Bmp7 may function through the intracellular formation of heterodimers.

In the case of heterodimer formation, cooperativity in our ventralizing assay system (Fig. 8) would depend on the coexpression of *bmp2b* and *bmp7* in the same cell, since heterodimers form intracellularly. However, if the synergy we observe is mediated by Bmp2b and Bmp7 homodimers, then a non-cell-autonomous interaction between these factors is expected. Both *swr/bmp2b* (Kishimoto et al., 1997; Nguyen et al., 1998b) and *snh/bmp7* (S. A. C. and M. C. M., unpublished) act in a non-cell-autonomous manner, although Bmp2b and Bmp4 may act only at short-range (Jones et al., 1996; Nikaido et al., 1999). Our finding that the synergy between *bmp2b* and *bmp7* depends on a cell-autonomous interaction between these factors, therefore strongly suggests that Bmp2b and Bmp7 cooperate by heterodimer formation.

In conclusion, our genetic analysis shows that *swr/bmp2b* and *snh/bmp7* play equivalent, non-redundant roles in dorsoventral pattern formation of the zebrafish embryo. Our experiments further suggest that Bmp2b and Bmp7 cooperate to specify ventral cell fates by forming heterodimers, in agreement with the fact that loss of function of either dimerization partner causes identical, strongly dorsalized mutant phenotypes.

REFERENCES

Aono, A., Hazama, M., Notoya, K., Taketomi, S., Yamasaki, H., Tsukuda, R., Sasaki, S. and Fujisawa, Y. (1995). Potent ectopic bone inducing activity of bone morphogenetic protein-4/7 heterodimer. *Biochem. Biophys. Res. Commun.* **210**, 670-677.

Arora, K., Levine, M. S. and O'Connor, M. B. (1994). The *screw* gene encodes a ubiquitously expressed member of the TGF-β family required for specification of dorsal cell fates in the *Drosophila* embryo. *Genes Dev.* **8**, 2588-2601.

Cho, K. W. Y. and Blitz, I. L. (1998). BMPs, Smads and metalloproteases: extracellular and intracellular modes of negative regulation. *Curr. Opin. Genet. Dev.* **8**, 443-449.

Connors, S. A., Trout, J., Ekker, M. and Mullins, M. C. (1999). The role of *tolloid/mini fin* in dorsoventral pattern formation of the zebrafish embryo. *Development* **126**, 3119-3130.

De Robertis, E. M. and Sasai, Y. (1996). A common plan for dorsoventral patterning in Bilateria. *Nature* **380**, 37-40.

Dudley, A. T., Lyons, K. M. and Robertson, E. J. (1995). A requirement for bone morphogenic protein-7 during development of the mammalian kidney and eye. *Genes Dev.* **9**, 2795-2807.

Dudley, A. T. and Robertson, E. J. (1997). Overlapping Expression Domains of Bone Morphogenetic Protein Family Members Potentially Account for Limited Tissue Defects in *BMP7* Deficient Embryos. *Dev. Dynam.* **208**, 349-362.

Ekker, M., Akimenko, M.-A., Allende, M. L., Smith, R., Drouin, G., Langille, R. M., Weinberg, E. S. and Westerfield, M. (1997). Relationships among *msx* gene structure and function in zebrafish and other vertebrates. *Mol. Biol. Evol.* **14**, 1008-1022.

Ferguson, E. (1996). Conservation of dorsal-ventral patterning in arthropods and chordates. *Curr. Opin. Gen. Dev.* **6**, 424-431.

Fritz, A., Rozowski, M., Walker, C. and Westerfield, M. (1996). Identification of selected gamma-ray induced deficiencies in zebrafish using multiplex polymerase chain reaction. *Genetics* **144**, 1735-1745.

Hawley, S. H. B., Wünnenberg-Stapleton, K., Hashimoto, C., Laurent, M. N., Watabe, T., Blumberg, B. W. and Cho, K. W. Y. (1995). Disruption of BMP signals in embryonic *Xenopus* ectoderm leads to direct neural induction. *Genes Dev.* **9**, 2923-2935.

Hazama, M., Aono, A., Ueno, N. and Fujisawa, Y. (1995). Efficient expression of a heterodimer of bone morphogenetic protein subunits using a baculovirus expression system. *Biochem. Biophys. Res. Commun.* **209**, 859-866.

Hild, M., Dick, A., Rauch, G. J., Meier, A., Bouwmeester, T., Haffter, P. and Hammerschmidt, M. (1999). The *smad5* mutation *somitabun* blocks Bmp2b signaling during early dorsoventral patterning of the zebrafish embryo. *Development* **126**, 2149-2159.

Hogan, B. L. (1996). Bone morphogenic proteins: mulitifunctional regulators of vertebrate development. *Genes Dev.* **10**, 1580-1594.

Israel, D. I., Nove, J., Kerns, K. M., Kaufman, R. J., Rosen, V., Cox, K. A. and Wozney, J. M. (1996). Heterodimeric Bone Morphogenetic Proteins Show Enhanced Activity *In Vitro* and *In Vivo*. *Growth Factors* **13**, 291-300.

Jones, C. M., Armes, N. and Smith, J. C. (1996). Signalling by TGF-β family members: short-range effects of Xnr-2 and BMP-4 contrast with the long-range effects of activin. *Curr. Biol.* **6**, 1468-1475.

Kim, J., Ault, K. T., Chen, H.-D., Xu, R.-H., Roh, D.-H., Lin, M. C., Park, M.-J. and Kung, H.-F. (1998). Transcriptional regulation of BMP-4 in the *Xenopus* embryo: analysis of genomic BMP-4 and its promoter. *Biochem. Biophys. Res. Commun.* **250**, 516-530.

Kishimoto, Y., Lee, K. H., Zon, L., Hammerschmidt, M. and Schulte-Merker, S. (1997). The molecular nature of zebrafish *swirl*: BMP2 function is essential during early dorsoventral patterning. *Development* **124**, 4457-4466.

Knapik, E. W., Goodman, A., Ekker, M., Chevrette, M., Delgado, J., Neuhauss, S., Shimoda, N., Driever, W., Fishman, M. C. and Jacob, H. J. (1998). A microsatellite genetic linkage map for zebrafish (*Danio rerio*). *Nat. Genet.* **18**, 338-343.

Krauss, S., Johansen, T., Korzh, V. and Fjose, A. (1991). Expression Pattern of Zebrafish pax Genes Suggests a Role in Early Brain Regionalization. *Nature* **353**, 267-270.

Massagué, J. (1998). TGFβ signal transduction. *Ann. Rev. Biochem.* **67**, 753-91.

Metz, A., Knöchel, S., Büchler, P., Köster, M. and Knöchel, W. (1998). Structural and functional analysis of the BMP-4 promoter in early embryos of *Xenopus laevis*. *Mech. Dev.* **74**, 29-39.

Mishina, Y., Suzuki, A., Ueno, N. and Behringer, R. R. (1995). Bmpr encodes a type I bone morphogenetic protein receptor that is essential for gastrulation during mouse embryogenesis. *Genes Dev.* **9**, 3027-3037.

Mullins, M. C., Hammerschmidt, M., Kane, D. A., Odenthal, J., Brand, M., van Eeden, F. J. M., Furutani-Seiki, M., Granato, M., Haffter, P., Heisenberg, C.-P. et al. (1996). Genes establishing dorsoventral pattern formation in the zebrafish embryo: the ventral specifying genes. *Development* **123**, 81-93.

Neul, J. L. and Ferguson, E. L. (1998). Spatially restricted activation of the SAX receptor by SCW modulates DPP/TKV signaling in *Drosophila* dorsal-ventral patterning. *Cell* **95**, 483-494.

Nguyen, M., Park, S., Marqués, G. and Arora, K. (1998a). Interpretation of a BMP activity gradient in *Drosophila* embryos depends on synergistic signaling by two type I receptors, SAX and TkV. *Cell* **95**, 495-506.

Nguyen, V. H., Schmid, B., Trout, J., Connors, S. A., Ekker, M. and Mullins, M. C. (1998b). Ventral and Lateral Regions of the Zebrafish Gastrula, Including the Neural Crest Progenitors, are Established by a *bmp2b/swirl* Pathway of Genes. *Dev. Biol.* **199**, 93-110.

Nikaido, M., Tada, M., Saji, T. and Ueno, N. (1997). Conservation of BMP signaling in zebrafish mesoderm patterning. *Mech. Dev.* **61**, 75-88.

Nikaido, M., Tada, M., Takeda, H., Kuroiwa, A. and Ueno, N. (1999). In vivo analysis using variants of zebrafish BMPR-IA: range of action and involvement of BMP in ectoderm patterning. *Development* **126**, 181-190.

Nishimatsu, S., Suzuki, A., Shoda, A., Murakami, K. and Ueno, N. (1992). Genes for Bone Morphogenic Proteins are differentially transcribed in early amphibian embryos. *Biochem. Biophys. Res. Commun.* **186**, 1487-1495.

Nishimatsu, S. and Thomsen, G. H. (1998). Ventral mesoderm induction and patterning by bone morphogenetic protein heterodimers in *Xenopus* embryos. *Mech. Dev.* **74**, 75-88.

Odenthal, J. and Nüsslein-Volhard, C. (1998). *fork head* domain genes in zebrafish. *Dev. Genes Evol.* **208**, 245-258.

Oezkaynak, E., Rueger, D. C., Drier, E. A., Corbett, C., Ridge, R. J., Sampath, T. K. and Oppermann, H. (1990). OP-1 cDNA encodes an osterogenic protein in the TGF-β family. *EMBO J.* **9**, 2085-2093.

Postlethwait, J. H., Yan, Y.-L., Gates, M. A., Horne, S., Ekker, M., Amores, A., Brownlie, A., Donovan, A., Egan, E. S., Force, A., et al. (1998). Vertebrate genome evolution and zebrafish gene map. *Nature Genet.* **18**, 345-349.

Schulte-Merker, S., Lee, K. J., McMahon, A. P. and Hammerschmidt, M. (1997). The zebrafish organizer requires *chordino*. *Nature* **387,** 862-863.

Solloway, M. J., Dudley, A. T., Bikoff, E. K., Lyons, K. M., Hogan, B. L. and Robertson, E. J. (1998). Mice lacking Bmp6 function. *Dev. Genet.* **22**, 321-339.

Solloway, M. J. and Robertson, E. J. (1999). Early embryonic lethality in *Bmp5; Bmp7* double mutant mice suggests functional redundancy within the 60A subgroup. *Development* **126**, 1753-1768.

Storm, E. E. and Kingsley, D. M. (1996). Joint patterning defects caused by single and double mutations in members of the bone morphogenetic protein (BMP)family. *Development* **122**, 3969-3979.

Suzuki, A., Kaneko, E., Maeda, J. and Ueno, N. (1997a). Mesoderm Induction by BMP-4 and -7 Heterodimers. *Biochem. Biophys. Res. Commun.* **232**, 153-156.

Suzuki, A., Kaneko, E., Ueno, N. and Hemmati-Brivanlou, A. (1997b). Regulation of Epidermal Induction by BMP2 and BMP7 Signaling. *Dev. Biol.* **189**, 112-122.

Thomas, J. T., Kilpatrick, M. W., Lin, K., Erlacher, L., Lembessis, P., Costa, T., Tsipouras, P. and Luyten, F. P. (1997). Disruption of human limb morphogenesis by a dominant negative mutation in *CDMP1*. *Nature Genet.* **17**, 58-64.

Wang, S., Krinks, M., Kleinwaks, L. and Moos Jr., M. (1997). A novel *Xenopus* homologue of bone morphogenetic protein-7 (BMP-7). *Genes Function* **1**, 259-271.

Weinberg, E. S., Allende, M. L., Kelly, C. L., Abdelhamid, A., Murakami, T., Andermann, P., Doerre, G., Grunwald, D. J. and Riggleman, B. (1996). Developmental regulation of zebrafish *MyoD* in wild-type, *no tail*, and *spadetail* embryos. *Development* **122**, 271-280.

Winnier, G., Blessing, M., Labosky, P. A. and Hogan, B. L. M. (1995). Bone morphogenetic protein-4 is required for mesoderm formation and patterning in the mouse. *Genes Dev.* **9**, 2105-2116.

Zhang, H. and Bradley, A. (1996). Mice deficient for BMP2 are nonviable and have defects in amnion/chorion and cardiac development. *Development* **122**, 2977-2986.